Inactivation Kinetics and Membrane Potential of Pathogens in Soybean Curd Subjected to Pulsed Ohmic Heating Depending on Applied Voltage and Duty Ratio

Eun-Rae Cho,[a] Sang-Soon Kim,[b] Dong-Hyun Kang[a,c]

[a]Department of Agricultural Biotechnology, Center for Food and Bioconvergence, and Research Institute for Agricultural and Life Sciences, Seoul National University, Seoul, Republic of Korea
[b]Department of Food Engineering, Dankook University, Cheonan, Chungnam, Republic of Korea
[c]Institutes of Green Bio Science and Technology, Seoul National University, Seoul, Republic of Korea

ABSTRACT The aim of this research was to investigate the efficacy of the duty ratio and applied voltage in the inactivation of pathogens in soybean curd by pulsed ohmic heating (POH). The heating rate of soybean curd increased rapidly as the applied voltage increased, although the duty ratio did not affect the temperature profile. We supported this result by verifying that electrical conductivity increased with the applied voltage. *Escherichia coli* O157:H7, *Salmonella enterica* serovar Typhimurium, and *Listeria monocytogenes* in soybean curd were significantly ($P < 0.05$) inactivated by more than 1 log unit at 80 V_{rms} (root mean square voltage). To elucidate the mechanism underlying these results, the membrane potential of the pathogens was examined using DiBAC$_4$(3) [bis-(1,3-dibutylbarbituric acid)trimethine oxonol] on the basis of a previous study showing that the electric field generated by ohmic heating affected the membrane potential of cells. The values of DiBAC$_4$(3) accumulation increased under increasing applied voltage, and they were significantly ($P < 0.05$) higher at 80 V_{rms}, while the duty ratio had no effect. In addition, morphological analysis via transmission electron microscopy showed that electroporation and expulsion of intracellular materials were predominant at 80 V_{rms}. Moreover, electrode corrosion was overcome by the POH technique, and the textural and color properties of soybean curd were preserved. These results substantiate the idea that the applied voltage has a profound effect on the microbial inactivation of POH as a consequence of not only the thermal effect, but also the nonthermal effect, of the electric field, whereas the duty ratio does not have such an effect.

IMPORTANCE High-water-activity food products, such as soybean curd, are vulnerable to microbial contamination, which causes fatal foodborne diseases and food spoilage. Inactivating microorganisms inside food is difficult because the transfer of thermal energy is slower inside than it is outside the food. POH is an adequate sterilization technique because of its rapid and uniform heating without causing electrode corrosion. To elucidate the electrical factors associated with POH performance in the inactivation of pathogens, the effects of the applied voltage and duty ratio on POH were investigated. In this study, we verified that a high applied voltage (80 V_{rms}) at a duty ratio of 0.1 caused thermal and nonthermal effects on pathogens that led to an approximately 4-log-unit reduction in a significantly short time. Therefore, the results of this research corroborate database predictions of the inactivation efficiency of POH based on pathogen control strategy modeling.

Address correspondence to Dong-Hyun Kang, kang7820@snu.ac.kr.

Soybean curd is produced by precipitating soybean proteins and calcium or magnesium salt, and it has abundant proteins, isoflavones, and antioxidants (1); therefore, it has been recognized as a health food that can prevent illnesses, such as stroke, ischemia, and cancer (2, 3). However, soybean curd has a neutral pH with abundant proteins and moisture, which are good conditions for microorganism growth (4). Thus, soybean curd can be easily contaminated by foodborne pathogens, such as *Escherichia coli* O157:H7, *Salmonella*, *Listeria* spp., and *Bacillus cereus*, during processing or distribution (5, 6). Ananchaipattana et al. (6) reported that foodborne pathogens, such as *B. cereus* and *Staphylococcus* spp., were detected in soybean curd in Thailand. Kwon et al. (7) also investigated the contamination level of *B. cereus* in packaged soybean curd at a retail market in South Korea and indicated that 12.9% of 85 samples were positive, with an average level of 1.84 log CFU/g. Several outbreaks of foodborne disease related to soybean curd have been reported. For instance, infections by *Yersinia enterocolitica* were related to contaminated soybean curd in Washington state (8). In March 2012, an outbreak associated with home-fermented soybean curd was reported and identified as foodborne botulism caused by eating foods contaminated with botulinum toxin (9). In addition, it was reported that 670 out of 918 people who ingested soybean curd (Sasayuki tofu) contaminated by enteroinvasive *E. coli* (EIEC) showed symptoms of diarrhea (93.4%), fever (77.5%), abdominal pain (64.5%), and vomiting (19.9%) (10). These food poisoning cases indicate that appropriate sterilization techniques are needed in the course of processing to ensure the microbiological safety of soybean curd.

The ohmic heating (OH) technique (Fig. 1) is a novel alternative to conventional heating for food processing, such as sterilization, cooking, thawing, and dehydration, because of the rapid and uniform heating, which retains the safety and high quality of foods (11, 12). OH generates thermal energy by passing an electric current through materials acting as electrical resistors. A power supply generates the electric current, which passes from the electric wire to an electrode and flows through an object between electrodes. When electricity flows through the substance, electric power (energy) is lost when electrons collide with other electrons, atoms, or neutrons, which is the so-called resistance loss (or ohmic loss) (13). Therefore, ohmic loss is converted into thermal energy, which raises the temperature of a material between electrodes uniformly and rapidly. OH technology induces fatal thermal damage and the formation of slight electroporation in a bacterial cell membrane, which leads to cell death due to leakage of cellular materials (14). There are many factors that affect the efficiency of OH, such as the applied voltage (voltage gradient), a material's electrical conductivity, and the frequency (11, 15). In the previous studies, inactivation efficacy against pathogens increased at a higher voltage gradient and frequency (16). In particular, OH at high frequencies of 10 kHz and 20 kHz prevented corrosion and elution of electrodes inactivating *E. coli* O157:H7, *Salmonella enterica* serovar Typhimurium, and *Listeria monocytogenes* effectively (17). With regard to voltage gradients, the temperature of the sample increased more rapidly when a high voltage gradient was applied, and the log reduction of pathogens was higher than with lower voltage gradients (16, 18).

Despite its advantages, the severe drawbacks of OH are the corrosion and leakage of electrode ions during treatment. In the above-mentioned research, the pulsed ohmic heating (POH) technique significantly reduced corrosion of electrodes by depleting the charged electrical double-layer capacitor, and then it impeded the faradaic current (19). High frequency is another preventive measure that obstructs the corrosion of electrodes by impeding full charging of the electrode double layers. In addition to preventing electrode corrosion by the POH technique, titanium is used as an electrode material because of its electrochemical corrosion resistance property and high stability (20–22), which minimize the corrosion of electrodes effectively during POH treatment. Therefore, POH with titanium electrodes is a relatively safe heating technique to sterilize or pasteurize food, reducing electrode corrosion.

Although considerable research has focused on the soybean curd production process by OH (23–25), research about the application of POH for inactivation against
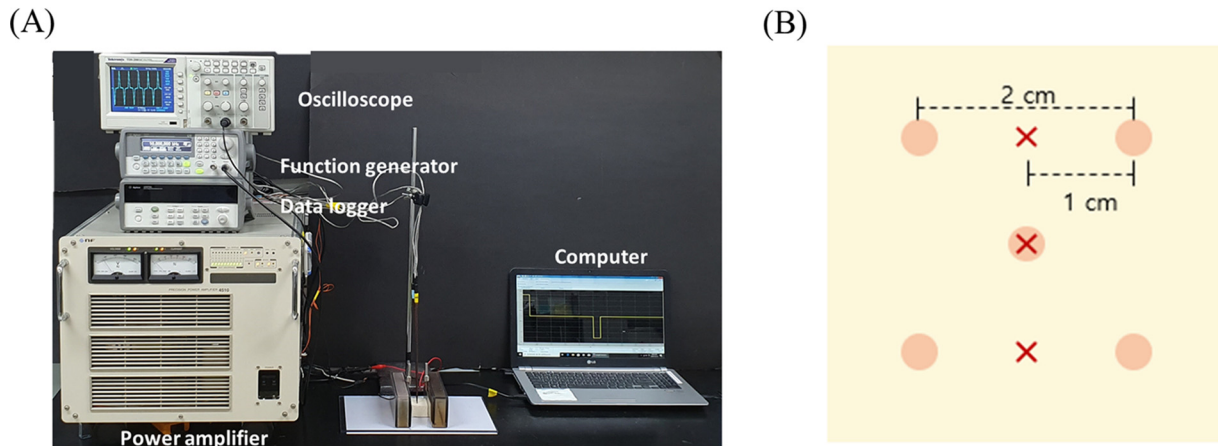
(A)

(B)

FIG 1 Pulsed ohmic heating system used in this research (A) and inoculation ($\times$) and temperature measurement (circles) points (B).

pathogens in soybean curd is limited. In addition, very few studies on POH have been applied to solid food products for the purpose of foodborne pathogen inactivation. Based on our previous research showing that the corrosion of electrodes could be depleted by POH at a duty ratio of 0.1 (19), this research investigated the efficacy of a POH system (Fig. 1) in inactivating *E. coli* O157:H7, *S.* Typhimurium, and *L. monocytogenes* inside soybean curd, depending on the duty ratio at 48 V_{rms} (root mean square voltage) and the voltage at a duty ratio of 0.1, and at preventing electrode corrosion. Furthermore, whether the field strength developed by POH influences membrane potential, using DiBAC$_4$(3) [bis-(1,3-dibutylbarbituric acid)trimethine oxonol], and electroporation of the cell membrane, depending on the duty ratio and applied voltage, were analyzed by transmission electron microscopy. This research may provide a basic database for predicting inactivation efficiency on the basis of modeling, with the aim of applying it in the food industry.

RESULTS

Temperature profile with regard to duty ratio and applied-voltage analysis. As shown in Fig. 2A, the temperature increased identically at duty ratios of 0.05 and 0.1 during POH treatment. Approximately 290, 340, 390, and 440 s were required to reach
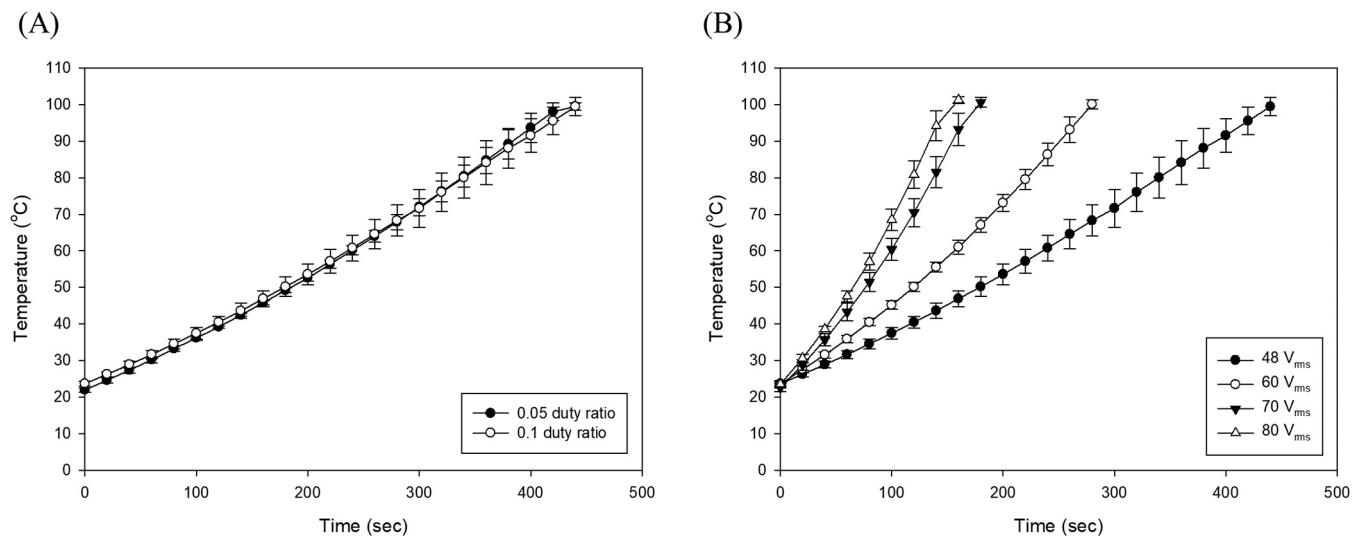
(A)

(B)

FIG 2 Temperature profile depending on the duty ratio at 48 V_{rms} (A) and applied voltage (V_{rms}) at 0.1 duty ratio (B) during POH treatment. The error bars represent standard deviations.

(A)

(B)

FIG 3 Electric current (in amperes) depending on the duty ratio at 48 V_{rms} (A) and applied voltage (V_{rms}) at 0.1 duty ratio (B) during POH treatment. The error bars represent standard deviations.
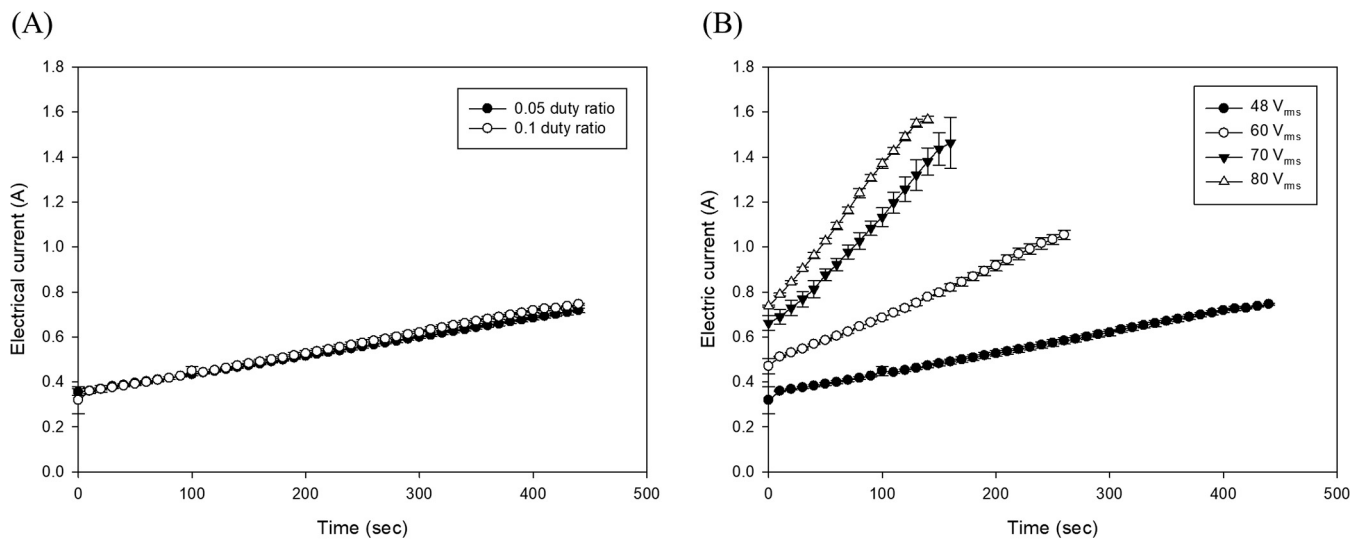
70, 80, 90, and 100°C, respectively, regardless of the duty ratio, when 48 V_{rms} was applied. Thus, the duty ratio exerted no significant influence on the rate of temperature rise. On the other hand, at the same duty ratio (0.1), the temperature of the sample increased rapidly over time as the applied voltage increased (Fig. 2B). Approximately 439, 280, 177, and 150 s were required to reach 100°C at 48, 60, 70, and 80 V_{rms}, respectively. The time intervals to increase the temperature by 10°C were 50, 30, 20, and 15 s at 48, 60, 70, and 80 V_{rms}. The heating rate was significantly ($P < 0.05$) increased by applying higher voltage, which means that the POH treatment time to reach the target temperature by means of an increased heating rate decreased noticeably.

Comparison of electric current and conductivity at different duty ratios and applied voltages. The electric current (in amperes [A]) curves of soybean curd at different duty ratios and applied voltages during POH treatment are shown in Fig. 3. The overall trend of the electric current increased almost linearly with increasing processing time and temperature. In this study, it was observed that the electric current increased equally when applying duty ratios of 0.05 and 0.1 at the same voltage (48 V_{rms}) (Fig. 3A). The maximum electric current values of 0.72 and 0.71 A were measured at duty ratios of 0.05 and 0.1 after 440 s of POH processing. Furthermore, the electric current values at different duty ratios were analogous to each other overall. Thus, the results indicate that there were no significant differences ($P > 0.05$) in the electric current of soybean curd over time between duty ratios of 0.05 and 0.1. However, it was observed that, as the applied voltage increased from 48 to 80 V_{rms}, the electric current increased simultaneously, as shown in Fig. 3B. The maximum electric current values depending on each applied voltage were 0.75, 1.05, 1.46, and 1.57 A at 48, 60, 70, and 80 V_{rms}, respectively, indicating that the electric current of the soybean curd increased significantly ($P < 0.05$) as the applied voltage increased.

The calculated electrical conductivity (in siemens [S] per meter) curves (see equation 3) are presented in Fig. 4. Similar to the electric current, the electrical conductivity trend is linear, depending on treatment time and temperature. When the temperature of the soybean curd reached 100°C during POH treatment, there were no significant differences in electrical conductivity between duty ratios of 0.05 and 0.1 (Fig. 4A). However, the electrical conductivity values were 0.52, 0.59, 0.70, and 0.65 S/m at 48, 60, 70, and 80 V_{rms} when samples treated by POH reached 100°C (Fig. 4B). Therefore, the electrical conductivity of soybean curd shows significantly higher values when higher applied voltages are exerted, although at 70 and 80 V_{rms}, they showed no significant difference ($P > 0.05$).
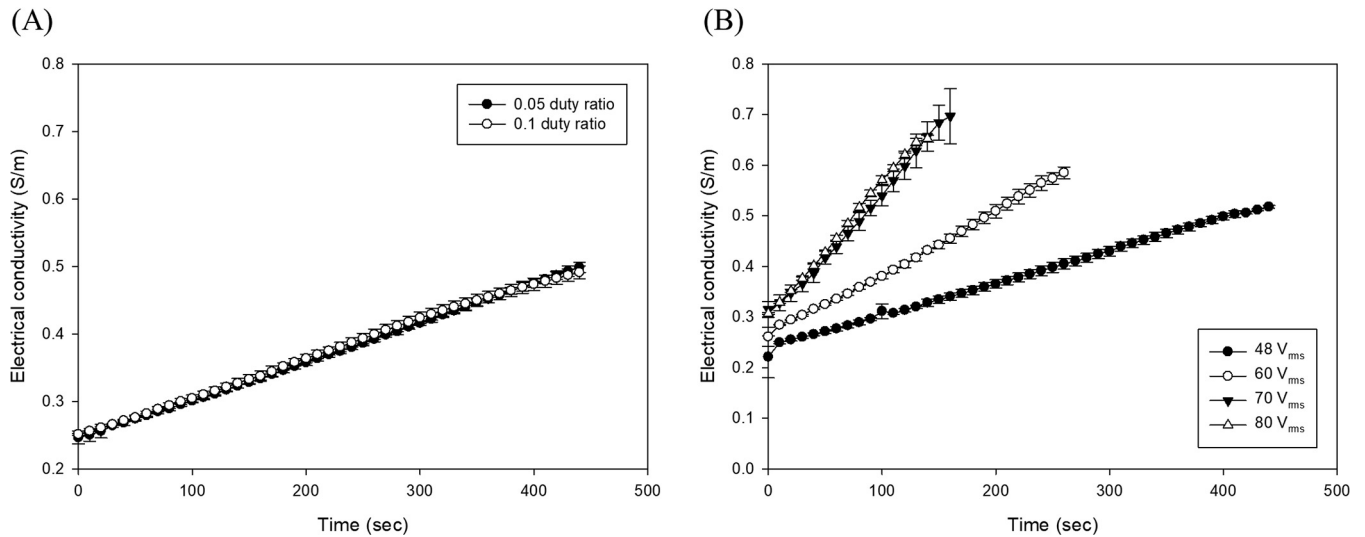
(A)

(B)

FIG 4 Electrical conductivity (in siemens per meter) depending on the duty ratio at 48 V_{rms} (A) and applied voltage (V_{rms}) at 0.1 duty ratio (B) during POH treatment. The error bars represent standard deviations.

Effects of duty ratio and applied voltage on inactivation of pathogens in soybean curd. The log reductions (log CFU per milliliter) of *E. coli* O157:H7, *S.* Typhimurium, and *L. monocytogenes* inoculated inside soybean curd at different duty ratios and different applied voltages are presented in Fig. 5 and 6. As shown in Fig. 5, except for the reduction of *E. coli* O157:H7 at 80 and 90°C, there was no significant difference in the reductions based on the duty ratio when 48 V_{rms} was applied ($P > 0.05$). The correlation between surviving populations of pathogens and applied voltage is presented in Fig. 6. In all pathogens, regardless of the applied-voltage, reduction of *E. coli* O157:H7, *S.* Typhimurium, and *L. monocytogenes* subjected to POH treatment tended to increase with increasing POH treatment time and temperature. When the holding time (HT) was added to the time it took to increase by 10°C after the temperature of samples reached 100°C (100 with HT), the reduction of pathogens subjected to POH at 80 V_{rms} was highest. After POH treatment for 160 s at 80 V_{rms}, 4.16-, 4.24-, and 3.99-log-unit reductions were observed in *E. coli* O157:H7, *S.* Typhimurium, and *L. monocytogenes*, respectively, which were more than 1 log unit higher than the results of other applied voltages. These results indicate that POH treatment at 80 V_{rms} has a significant effect on the inactivation of each pathogen when samples are treated until they reach over 100°C.

Kinetics modeling of inactivation of pathogens. Survival curves were fitted to the Weibull model (see below) to compare T_{3d} and T_{5d}, which represent the times required to achieve 3- and 5-log-unit reductions, respectively. As shown in Table 1, all regression coefficient values (R^2), which indicate the best fit to the acquired data that is close to 1, showed values of more than 0.90. Additionally, root mean square error (RMSE) values between 0.17 and 0.45 were obtained. The lower the RMSE value, the better the Weibull model fits the data (26). All the survival population curves of pathogens correspond to convex shapes, because the ρ values were calculated at more than 1 (27). The δ values of *S.* Typhimurium and *L. monocytogenes* were not significantly different from those at 0.1 and 0.05 duty ratios at 48 V_{rms}. Regarding the results of the δ values of pathogens depending on the applied voltage, the values of all pathogens tended to increase as applied voltage increased. Except for the case of *L. monocytogenes* subjected to 48-V_{rms} POH at a duty ratio of 0.1, all T_{5d} values were significantly higher than the T_{3d} values ($P < 0.05$). When the T_{3d} and T_{5d} values under each different applied voltage condition at the same duty ratio were compared, both values were reduced as the applied voltage increased. In particular, T_{3d} values were shortened by approximately 3.98-, 3.61-, and 3.31-fold for *E. coli* O157:H7, *S.* Typhimurium, and *L. monocytogenes*, respec-
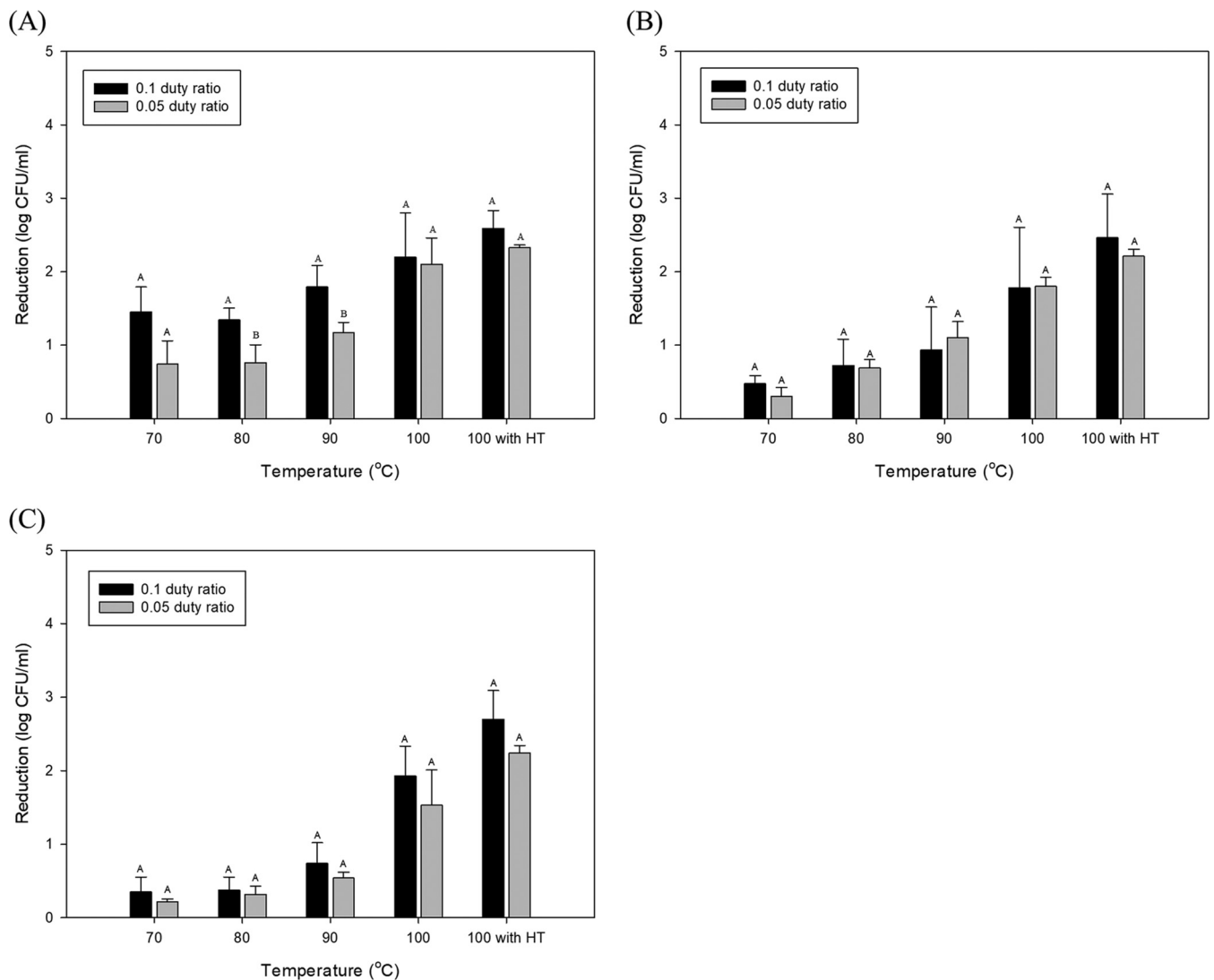
(A)

(B)

(C)

FIG 5 Reduction (log CFU per milliliter) of *E. coli* O157:H7 (A), *S.* Typhimurium (B), and *L. monocytogenes* (C) inoculated on samples after 48-V_{rms} POH treatment at duty ratios of 0.05 and 0.1. The error bars represent standard deviations. Different uppercase letters for the same treatment temperature indicate a significant difference ($P < 0.05$).

tively, by increasing the voltage from 48 to 80 V_{rms}. Additionally, the T_{5d} values were shortened 4.75-, 3.40-, and 3.14-fold for *E. coli* O157:H7, *S.* Typhimurium, and *L. monocytogenes*, respectively, by increasing the voltage from 48 to 80 V_{rms}.

Evaluation of cell membrane damage and potential by DiBAC$_4$(3). The DiBAC$_4$(3) relative accumulation ratio, which is presented as the percentage for the treatment group relative to the control group, is presented in Table 2. The duty ratio did not exert a significant effect ($P > 0.05$) on the relative ratio values for *E. coli* O157:H7 and *L. monocytogenes*, although it had a significant ($P < 0.05$) effect on values for *S.* Typhimurium. The ratios were highest for *E. coli* O157:H7, followed by *S.* Typhimurium and *L. monocytogenes*. However, when the results according to each applied voltage were compared, the DiBAC$_4$(3) values increased with increases in applied voltage. In particular, the ratios were significantly ($P < 0.05$) higher for all the pathogens when 80 V_{rms} was applied. A comparison of the pathogens showed that *E. coli* O157:H7 had significantly ($P < 0.05$) higher values than the other pathogens at 48 and 60 V_{rms}. On the other hand, the values for *S.* Typhimurium were significantly ($P < 0.05$) higher than those for the other pathogens at 70 and 80 V_{rms}.
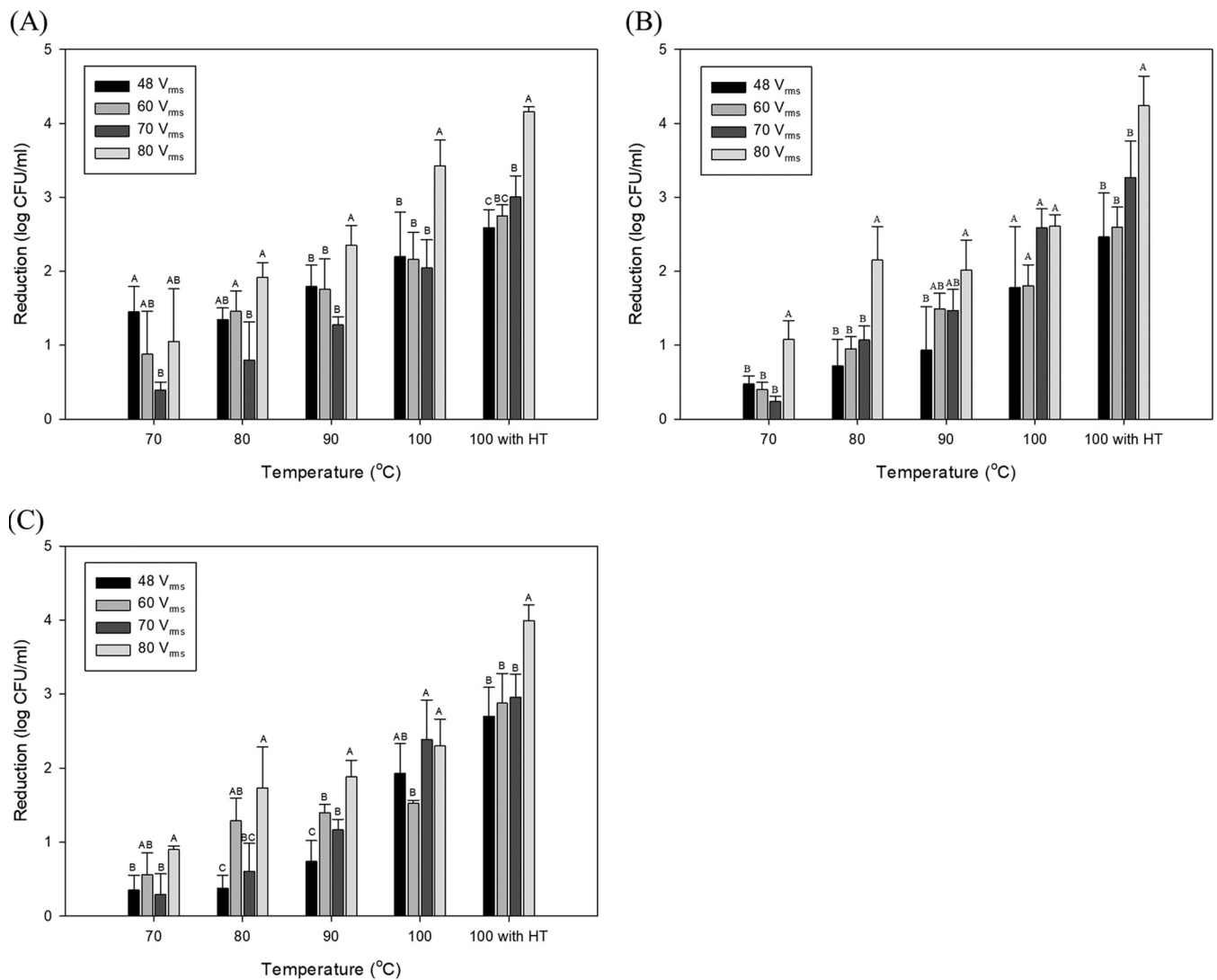
FIG 6 Reduction (log CFU per milliliter) of *E. coli* O157:H7 (A), *S.* Typhimurium (B), and *L. monocytogenes* (C) inoculated on samples after POH treatment at different applied voltages at 0.1 duty ratio. The error bars represent standard deviations. Different uppercase letters for the same treatment temperature indicate a significant difference ($P < 0.05$).

Transmission electron microscopy. As shown in Fig. 7, cells subjected to POH under each condition were examined under a transmission electron microscope (TEM). Although the morphologies of the pathogens showed slightly disrupted cell membranes and trace amounts of cellular material eruption at duty ratios of 0.1 and 0.05 at 48 V_{rms} (Fig. 7B and C), the disruption was not remarkable. Additionally, the cells subjected to POH at 60 V_{rms} did not show morphology significantly different from that at 48 V_{rms}. Meanwhile, a morphological difference in the cell membrane and expulsion of internal cellular materials were observed when the cells were treated by POH at 70 and 80 V_{rms} (Fig. 7E and F). Fatal disintegration of the cell membrane and intracellular material efflux was most critical at 80 V_{rms}. These results corresponded to those for the reduction and cell membrane potential/damage analysis using DiBAC$_4$(3).

Assessment of texture and color properties of soybean curd after POH treatment. Tables 3 and 4 list the texture properties and color values, respectively, of soybean curd after POH treatment. Excluding cohesiveness, all the texture properties of the samples treated with the POH process were not significantly ($P > 0.05$) different from those of untreated samples. The cohesiveness of soybean curd subjected to POH at 48 V_{rms} under a 0.05 duty ratio for 490 s was reduced by 0.11 compared to the

TABLE 1 Weibull modeling of *E. coli* O157:H7, *S.* Typhimurium, and *L. monocytogenes* inactivation in soybean curd[a]

Strain	Duty ratio	Applied voltage (V_{rms})	Log N_0 (log CFU/ml)	ρ	R^2	RMSE	δ (s)	T_{3d} (s)	T_{5d} (s)
E. coli O157:H7	0.05	48	8.15	2.69	0.9446	0.2500	348.40 ± 26.78 a	533.98 ± 23.71 Ba	653.28 ± 64.24 Ab
	0.1	48	8.06	1.39	0.9575	0.2402	252.76 ± 47.61 b	556.20 ± 52.23 Ba	804.63 ± 51.78 Aa
		60	8.00	2.11	0.9155	0.3705	189.02 ± 18.37 c	320.99 ± 1.62 Bb	411.63 ± 22.16 Ac
		70	8.16	3.96	0.9724	0.2408	148.81 ± 11.58 c	199.82 ± 2.66 Bc	229.56 ± 11.58 Ad
		80	8.24	2.61	0.9752	0.2937	91.42 ± 10.15 d	139.45 ± 4.32 Bd	169.96 ± 2.07 Ad
S. Typhimurium	0.05	48	7.33	3.15	0.9700	0.1777	372.89 ± 8.36 a	529.55 ± 4.58 Ba	623.47 ± 13.26 Aa
	0.1	48	7.23	4.59	0.9485	0.2454	389.40 ± 61.46 a	508.94 ± 23.54 Ba	577.97 ± 6.66 Ab
		60	6.89	3.11	0.9592	0.2255	226.07 ± 10.46 b	324.25 ± 6.45 Bb	383.83 ± 19.58 Ac
		70	7.64	3.46	0.9536	0.3292	138.66 ± 6.97 c	191.91 ± 4.00 Bc	223.45 ± 11.58 Ad
		80	7.35	2.52	0.9376	0.4457	92.96 ± 2.74 c	143.97 ± 3.78 Bd	176.48 ± 6.03 Ae
L. monocytogenes	0.05	48	8.54	5.34	0.9557	0.2233	416.67 ± 18.67 a	513.10 ± 9.10 Ba	565.38 ± 7.67 Aa
	0.1	48	8.58	5.04	0.9540	0.2788	394.30 ± 24.19 a	500.61 ± 18.50 Aa	560.51 ± 44.02 Aa
		60	8.42	3.07	0.9195	0.3563	226.12 ± 12.80 b	324.24 ± 8.36 Bb	385.75 ± 11.16 Ab
		70	8.67	3.99	0.9589	0.3028	148.02 ± 10.84 c	196.62 ± 3.77 Bc	224.58 ± 6.70 Ac
		80	8.59	3.30	0.9334	0.4115	106.03 ± 11.35 d	150.11 ± 1.94 Bd	176.80 ± 5.34 Ad

[a]Data are expressed as means ± standard deviations from three replications. Values followed by different uppercase letters in the same row are significantly different ($P < 0.05$). Values followed by different lowercase letters in the same column are significantly different ($P < 0.05$).

control. With respect to the color values of soybean curd after POH, the values of $L*$, $a*$, and $b*$ (see below) were not significantly different ($P > 0.05$) from those for the untreated samples.

Electrode corrosion measurement. The concentrations of eluted titanium ions in samples after POH are presented in Table 5. The concentration of migrated titanium ions was not detected under all conditions, except for samples treated by POH at 60 V_{rms} at a duty ratio of 0.1. When the POH treatment was operated at 60 V_{rms}, 0.02 ppm of titanium ions in the samples was detected.

DISCUSSION

The principal objectives of this study were to (i) investigate the optimal electrical conditions of POH for the nonthermal effect in order to inactivate pathogens in soybean curd and (ii) validate that the POH technique prevents electrode corrosion. The fundamental principle of the POH technique, which is operated by triggering a pulsed waveform, is to heat food products using thermal energy caused by the electrical resistance generated when passing an electric current directly through them. In general, much previous research has shown that OH has nonthermal bactericidal effects in addition to thermal effects. Somavat et al. (28) reported that when tomato juice samples inoculated with *Bacillus coagulans* spores were treated by ohmic and conventional heating, the D values (time required to reduce the microbial population by 1 log cycle at a specific temperature) for ohmic heating at 60 Hz and 10 kHz were significantly

TABLE 2 DiBAC$_4$(3) accumulation values[a]

Duty ratio	Applied voltage (V_{rms})	DiBAC$_4$(3) accumulation value (%) in[b]:		
		E. coli O157:H7	*S.* Typhimurium	*L. monocytogenes*
0.05	48	168.96 ± 4.87 Acd	133.49 ± 0.71 Be	126.18 ± 2.65 Cd
0.1	48	163.92 ± 4.92 Ad	140.79 ± 1.89 Bd	128.57 ± 3.02 Cd
	60	174.11 ± 1.35 Abc	162.73 ± 2.85 Bc	133.55 ± 1.54 Cc
	70	179.70 ± 3.92 Bb	187.77 ± 4.72 Ab	144.64 ± 0.88 Cb
	80	190.60 ± 0.93 Ba	202.09 ± 3.52 Aa	181.03 ± 2.60 Ca

[a]Values are presented as the ratio of each treatment group to the control for *E. coli* O157:H7, *S.* Typhimurium, and *L. monocytogenes* isolates treated by POH at different duty ratios and applied voltages for the maximum treatment times. Maximum treatment times were 490, 310, 200, and 160 s at 48, 60, 70, and 80 V_{rms}, respectively.
[b]Data are expressed as means ± standard deviations from three replications. Values followed by different uppercase letters in the same row are significantly different ($P < 0.05$). Values followed by different lowercase letters in the same column are significantly different ($P < 0.05$).
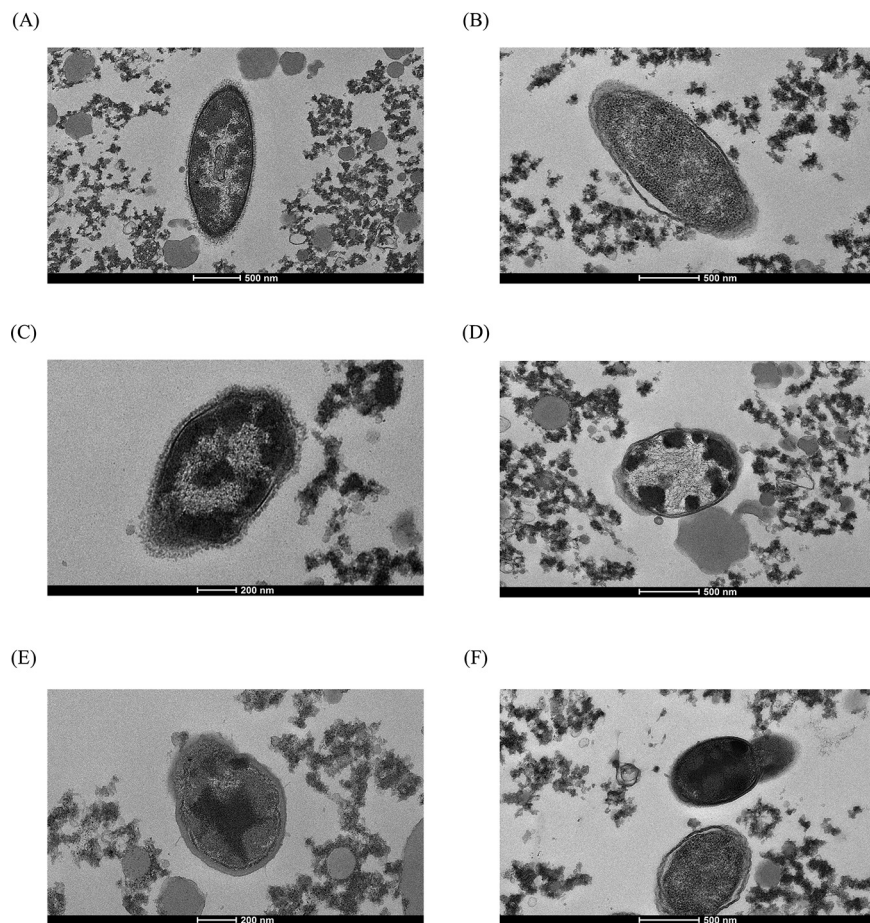
(A)

(B)

(C)

(D)

(E)

(F)

FIG 7 TEM microphotograph of pathogen cells that were not subjected (A) or subjected (B to F) to the POH process. The cells were treated at duty ratios of 0.05 (B) and 0.1 (C) under the same applied voltage (48 V$_{rms}$) and at 60 V$_{rms}$ (D), 70 V$_{rms}$ (E), and 80 V$_{rms}$ (F) under the same duty ratio (0.1). Treatment times were 490, 310, 200, and 160 s at 48, 60, 70, and 80 V$_{rms}$, respectively.

lower than those for conventional heating because of the nonthermal effects. Additionally, according to Sun et al. (29), OH caused nonthermal damage to *Streptococcus thermophilus*, as well as thermal damage. They conjectured that OH under appropriate conditions, such as electric current and frequency, could result in permeability of the cell membrane and concluded that OH has a nonthermal effect of the electric current. Therefore, the POH technique is an alternative sterilization process to conventional heating for inactivation of pathogens.

The cardinal factors affecting the OH process and heating rate included electrical conductivity, voltage, field strength (voltage gradient), electric current and ionic concentration, and electrode design (15, 30, 31). The optimal electrical conductivities of

TABLE 3 Texture properties of soybean curd subjected to POH for the maximum treatment times under different duty ratios and applied voltages[a]

Duty ratio	Applied voltage (V$_{rms}$)	Hardness (N)	Cohesiveness	Springiness (N·s)	Gumminess (N)	Chewiness (N)	Resilience
Control	Control	22.32 ± 3.10 A	0.49 ± 0.04 A	0.91 ± 0.04 A	11.00 ± 1.87 A	9.93 ± 1.36 A	0.36 ± 0.15 A
0.05	48	23.37 ± 2.63 A	0.38 ± 0.05 B	0.92 ± 0.09 A	9.06 ± 2.22 A	8.34 ± 2.08 A	0.36 ± 0.25 A
0.1	48	23.53 ± 0.54 A	0.40 ± 0.05 AB	0.87 ± 0.04 A	9.41 ± 1.30 A	8.19 ± 1.48 A	0.22 ± 0.14 A
	60	24.72 ± 0.26 A	0.41 ± 0.08 AB	0.92 ± 0.07 A	10.11 ± 1.79 A	9.26 ± 1.71 A	0.35 ± 0.23 A
	70	23.04 ± 1.74 A	0.41 ± 0.02 AB	1.19 ± 0.45 A	9.32 ± 0.50 A	11.20 ± 4.65 A	0.38 ± 0.23 A
	80	24.98 ± 3.51 A	0.45 ± 0.05 AB	0.95 ± 0.08 A	11.10 ± 1.80 A	10.46 ± 0.89 A	0.38 ± 0.25 A

[a]Maximum treatment times were 490, 310, 200, and 160 s at 48, 60, 70, and 80 V$_{rms}$, respectively. The data are expressed as means ± standard deviations from three replications. Values followed by the same uppercase letter in the same column are not significantly different ($P > 0.05$).

TABLE 4 Color values of soybean curd subjected to POH for the maximum treatment times under different duty ratios and applied voltages[a]

Duty ratio	Applied voltage (V_{rms})	$L*$	$a*$	$b*$
Control	Control	78.77 ± 0.40 A	−1.56 ± 0.10 A	11.47 ± 0.39 A
0.05	48	79.19 ± 0.28 A	−1.58 ± 0.04 A	11.41 ± 0.51 A
0.1	48	78.87 ± 0.14 A	−1.48 ± 0.05 A	11.60 ± 0.33 A
	60	79.31 ± 0.53 A	−1.59 ± 0.07 A	11.48 ± 0.31 A
	70	79.16 ± 0.57 A	−1.56 ± 0.08 A	11.31 ± 0.12 A
	80	78.15 ± 1.39 A	−1.60 ± 0.05 A	11.64 ± 0.42 A

[a]The maximum treatment times were 490, 310, 200, and 160 s at 48, 60, 70, and 80 V_{rms}, respectively. The data are expressed as means ± standard deviations from three replications. Values followed by the same uppercase letter in the same column are not significantly different ($P > 0.05$).

food products for OH treatment are 10 S/m and above 0.01 S/m (32, 33). Additionally, the electrical conductivities for food products are classified into three groups, where a σ value of >0.05 S/m is defined as good conductivity (12). As shown in Fig. 4, the electrical conductivity of soybean curd was above 0.25 and below 0.70 S/m at all applied voltages; therefore, it has suitable conductivity for the POH process.

The results of this study demonstrated that the duty ratio at the same applied voltage does not significantly affect the temperature profile, the electrical properties of soybean curd, and inactivation kinetics against pathogens; however, the specific applied voltage at the same duty ratio had a significant influence on the properties of POH. With regard to the temperature profile, the temperature increased equally when 48 V_{rms} was applied at duty ratios of 0.05 and 0.1, whereas it increased rapidly as the applied voltage increased and was 2.75 times faster at 80 V_{rms} than at 48 V_{rms} (Fig. 2). This means that the rate of temperature rise was significantly ($P < 0.05$) higher when a higher voltage was applied. Therefore, the heating rate showed voltage-dependent behavior, although the duty ratio did not. The applied voltages in this study could be converted to electric field strength or voltage gradient by dividing the distance between two electrodes (12, 15, 17.5, and 20 V/cm). In terms of the electric field strength, the rate of temperature rise at high electric field strength was significantly ($P < 0.05$) higher than that at lower electric field strength. Previous studies have also reported that the rate of temperature rise is proportional to the electric field strength or voltage gradient (34, 35). According to the results of Darvishi et al. (36), the time for heating tomato paste decreased from 235 to 38 s with voltage gradient increases from 6 to 14 V/cm. Additionally, Bozkurt and Icier (37) reported that the time to reach 100°C decreased with an increase in the voltage gradient from 10 to 30 V/cm. For this reason, it could be concluded that the heating rate is proportional to the electric field strength/voltage gradient. This phenomenon could also be delineated in accordance with Joule's law, expressed by equation 1:

$$Q = RI^2 t = VIt \qquad (1)$$

where Q is the amount of generated heat (J), R is the value of the electrical resistance of material (Ω), I is the electric current that flows through a material, t is the POH operating time (s), and V is the voltage applied to a material (V_{rms}) (38).

According to this equation, the amount of heat release is commensurate with the

TABLE 5 Titanium concentrations in soybean curd subjected to POH treatment under each condition for the maximum treatment times[a]

Duty ratio	Applied voltage (V_{rms})	Titanium concn (ppm)
0.05	48	ND[b]
0.1	48	ND
	60	0.02 ± 0.11
	70	ND
	80	ND

[a]Data are expressed as means ± standard deviations from three replications. The maximum treatment times were 490, 310, 200, and 160 s at 48, 60, 70, and 80 V_{rms}, respectively.
[b]ND, not detected.

square of the electric current and applied voltage. Thus, higher voltage and electric current generate more thermal energy that heats a material than lower voltage and electric current (39). In this study, it was observed that as the applied voltage increased, the electric current increased simultaneously, which is shown in Fig. 3B. However, the electric current increased equally at duty ratios of 0.05 and 0.1; hence, the quantity of the generated heat was consistent over time.

Another pivotal factor that has an influence on the temperature profile of POH is the electrical conductivity (in siemens per meter), which is a rudimentary material property that determines how well a material transmits, or conducts, electric current. There was no considerable difference in electrical conductivity between the duty ratios of 0.05 and 0.1, although the applied voltage affected electrical conductivity (Fig. 3). As shown in Fig. 3, it was observed that electrical conductivity increased linearly in proportion to the temperature over POH operation time because movement of ionic and polar substances, such as sodium ion, amino acid, and water, becomes more conspicuous with increases of temperature. The relationship between the electrical conductivity and temperature profile in other studies using solid food samples showed the same trend presented in this study (40–42). We suggest that (i) the applied voltage governs soybean curd's temperature profile during POH treatment, rather than the duty ratio, and (ii) the voltage, electric current, and conductivity were the main factors affecting the heating rate in this study.

Although inoculated samples were exposed to heat treatment by POH over a shorter time at 80 V_{rms} than at 48, 60, and 70 V_{rms} (the treatment time intervals were 15, 20, 30, and 50 s, respectively), the reduction of pathogens was more than 1 log unit at 80 V_{rms} compared with those at 48, 60, and 70 V_{rms} (Fig. 5). In other words, inactivation was more effective at 80 V_{rms} than at the other applied voltages, although the times of heat generation and internal heat gain were shorter because of the high heating rate. This means that thermal and nonthermal effects consisting of the electric field and electric current had a synergistic effect on the bactericidal ratio for pathogens inoculated into soybean curd. In accordance with previous research, the cardinal factors of OH for microbial inactivation were the electric field and electric current (33). Pereira et al. (43) showed that the reason that the D and Z values (the Z value is the increase in temperature required to attain a 1-log reduction in the D value) of *E. coli* ATCC 25922 subjected to OH were lower than those for conventional heating could be related to the electric field. In terms of electric current, in the study of Sun et al. (44), sterilized skim milk samples inoculated with *S. thermophilus* strain 2646 were subjected to OH and conventional heating to the target temperature, and they showed that the reductions of *S. thermophilus* treated by OH was much higher than that under conventional heating to the same temperature because of nonthermal effects as well as thermal effects. They supposed that the electric current has an influence on microbial inactivation based on a comparison of the survival population curves for OH and conventional heating. In this study, it was observed that the higher electric field strength and current increased the rate of pathogen inactivation (Fig. 3B and 6). Therefore, we deduced that POH at high applied voltage could effectively inactivate *E. coli* O157:H7, *S.* Typhimurium, and *L. monocytogenes* due to the electric field and current.

In regard to inactivation kinetics by Weibull modeling (Table 1), the time to the first log reduction of the initial population was inclined to decrease with applied voltage increase regardless of the strain. When the δ values of the pathogens were compared, *L. monocytogenes* was the highest, which means *L. monocytogenes* is more resistant to early treatment than *E. coli* O157:H7 and *S.* Typhimurium when subjected to POH treatment. The T_{3d} and T_{5d} values of *E. coli* O157:H7, *S.* Typhimurium, and *L. monocytogenes* prominently decreased as the applied voltage increased. The POH at 80 V_{rms} could inactivate pathogens efficiently in a short time. However, three strains showed similar T_{5d} values, which were 170, 176, and 177 s for *E. coli* O157:H7, *S.* Typhimurium, and *L. monocytogenes*, respectively. It was demonstrated that the thermal effect is a predominant factor in microbial inactivation by OH (12, 33). Heat induces damage to the cell membrane, enzymes, cellular organelles, etc., by denaturing proteins, which is

caused by disrupting hydrogen bonds and hydrophobic interactions. Thus, it is surmised that not only the cell membrane, but also DNA and other organelles, were damaged by heat generated by POH, so the T_{5d} of the pathogens tended to be similar without distinction of strain after the temperature of the sample reached 100°C. On the basis of these results, we could extrapolate that in the case of inactivation of pathogens in soybean curds, the minimum applied voltage for generating a prominent nonthermal disinfection effect is 80 V_{rms}.

To investigate the mechanism underlying microbial inactivation by POH, the transmembrane potential of the cell was measured using $DiBAC_4(3)$ (45, 46), an ionic fluorescent dye that is sensitive to voltage, and the results were used to evaluate cell membrane damage in the research. Several previous studies indicated that the external electric field exerts an influence on the membrane potential (47–50). Membrane potential is essential for the physiological functions of microorganism, such as metabolism, growth, and homeostasis, and it is involved in ATP synthesis; moreover, membrane transport regulates ion concentrations between the outside and inside of the cell (51–53). When the membrane potential is disturbed by physicochemical reactions, depolarization of the cell membrane occurs, and the interior of the cell and plasma membrane are more positively charged than those of a normal cell. The cell membrane becomes positive or depolarized and causes an influx of $DiBAC_4(3)$ into the cell; therefore, the fluorescent signal is maximized (54, 55). On the basis of this theoretical background, a degree of cell membrane intactness and inactivation of pathogens could be measured indirectly through an analysis of the $DiBAC_4(3)$ accumulation ratio. The results shown in Table 2 indicate that POH treatment at 80 V_{rms} at a duty ratio of 0.1 induced depolarization of the cell membrane and significantly high inactivation of pathogens ($P < 0.05$), as the data showed that the $DiBAC_4(3)$ accumulation ratio was highest ($P < 0.05$) at 80 V_{rms}. According to Sastry's description (56), OH causes a charge to be accumulated at the surface of the cell and leads to pore formation, which is known as electroporation. Donsì et al. (57) reported that when a biological cell is subjected to the threshold of the electric field, a critical membrane potential can be induced. Accumulated charges disturb the voltage gradient of the cell between the external and internal areas; therefore, the shape of the cell membrane becomes more variable and separate, and the membrane eventually collapses (49). Consequently, irreversible pores (electroporation) in the cell membrane are induced by the electric field. Moreover, a comparison of the $DiBAC_4(3)$ accumulation ratio and electric current, which is the rate of electrical charge, shows that the POH process at 80 V_{rms} provokes enough electric field and current to disrupt the membrane potential, resulting in a significant depolarization of transmembrane potential.

Meanwhile, as shown Table 2, the ratio of $DiBAC_4(3)$ accumulation for *L. monocytogenes* was significantly ($P < 0.05$) lower than those for *E. coli* O157:H7 and *S.* Typhimurium under all conditions. This result could indicate that the morphological and biochemical properties, such as the cell size and cell membrane, of microorganisms have an effect on the threshold value of the electric field strength, which is based on the research of Hülsheger et al. (48). A comparison between Gram-positive (*L. monocytogenes*) and Gram-negative (*E. coli* O157:H7 and *S.* Typhimurium) bacteria showed that the ratio of $DiBAC_4(3)$ accumulation for *L. monocytogenes* was significantly lower ($P < 0.05$) than those for *E. coli* O157:H7 and *S.* Typhimurium. This result could indicate that Gram-positive bacteria have more resistance to the electric field developed by POH. The results of this study correspond to those of Lee et al. (58), who reported that *L. monocytogenes*, a Gram-positive bacterium, has more resistance to OH than Gramnegative bacteria. Additionally, previous research (59) showed that the inactivation level of *Staphylococcus aureus* was lower than that of *E. coli*, and the authors explained that Gram-negative bacteria have much thinner peptidoglycan layers than Grampositive bacteria. These phenomena suggest that Gram-positive bacteria have a thick peptidoglycan layer on the outside of the plasma membrane; therefore, the bacteria have higher resistance to physical disruption, such as heat, drying, and permeation of reactive oxygen species (ROS) from plasma, than Gram-negative bacteria (60, 61). Thus,

the thick peptidoglycan layer permits Gram-positive bacteria to withstand the membrane damage caused by the thermal effect, as well as membrane potential disturbance from the external electric field. In summary, when cells are treated by POH at 80 V_{rms}, the exterior of the cell membrane facing the anode of the electrode becomes negatively charged above the threshold and the interior is positively charged, while in the cathode of the electrode, the phenomenon is reversed over the threshold; therefore, the cell is depolarized. For this reason, it was confirmed that the $DiBAC_4(3)$ accumulation ratio under 80 V_{rms} was significantly higher than that for other applied voltages.

To demonstrate the degrees of inactivation of pathogens, cell membrane rupture, and electroporation, which is optically dependent on the duty ratio and applied voltage, a TEM analysis was conducted. Studies have compared TEM micrographs of cells after OH and conventional heating treatment (14, 62, 63). For example, Lee et al. (63) examined the morphological structure of *E. coli* O157:H7 using TEM and found that the structure of the cell treated by OH at 30 V/cm for 180 s was significantly more collapsed than that under conventional heating due to electroporation. However, only one study performed a TEM analysis based on the duty ratio and voltage. The TEM microphotographs obtained in the present study revealed that a duty ratio at the same applied voltage had no effect on the morphological structure of pathogen cells, while the applied voltage, especially at 80 V_{rms}, significantly disrupted the integrity of the cell structure because the electric field and current contributed to membrane depolarization and electroporation, as indicated above. Additionally, it was observed that greater leakage of intracellular materials occurred through the ruptured pores of the cell membrane after POH treatment at 80 V_{rms}. This leakage of intracellular materials is another mechanism for microbial inactivation (64). To summarize the discussion of TEM microphotographs, this study morphologically demonstrates that POH at higher applied voltages leads to greater electroporation (electropermeabilization) and eruption of intracellular materials, which causes a greater reduction of pathogens.

After sterilization of soybean curd, maintaining the original qualities, such as color, texture, and nutrients, should not be overlooked because these qualities affect consumer acceptance (65). Kamizake et al. (66) reported that consumer acceptance declined when researchers provided soybean curd with a gray color and fracturable texture made from aged cultivars. According to a study by Obatolu (67), sensory scores for soybean curds made from different coagulants were influenced by color and textural attributes. For this reason, this study examined the texture properties based on a texture profile analysis (TPA) and color values. TPA is an imitative test for analyzing the rheological properties of materials, such as texture, and it is performed by compressing a sample twice, similar to a masticatory movement. In this study, the cohesiveness of soybean curd decreased significantly ($P < 0.05$) after POH treatment under an adjusted duty ratio of 0.05 at 48 V_{rms} for 490 s. Cohesiveness, calculated by dividing the area under the TPA curve during the first bite from that for the second bite, represents a textural property relevant to the degree to which a food can be deformed before it breaks (68) or a sample deforms before it ruptures (69). Additionally, Szczesniak (70) defined cohesiveness as "the strength of the internal bonds making up the body of the product." Thus, it is speculated that the internal bonds of soybean curd weakened after the POH process at 48 V_{rms} under a duty ratio of 0.05 due to the long treatment time (490 s) above 100°C. In previous research, sulfhydryl groups of soybean protein in tofu gel made from soy milk that was heated for a long time were oxidized and showed a soft texture (71). A study conducted by Furukawa et al. (72) showed that the cohesiveness of the isolated soy protein began to decrease at 100°C. They indicated that this phenomenon was due to the fact that excess heat effectuates chemical degradation of cysteine residues of proteins, which leads to unstable hydrogen and hydrophobic bonds. Based on these previous research studies, the cohesiveness of soybean curd decreased after POH treatment at 48 V_{rms} under a duty ratio of 0.05 for 490 s because excess heat weakens internal molecular bonds. Meanwhile, there were no significant ($P > 0.05$) differences in color in comparisons of nontreated and treated samples. Several studies also showed that OH could maintain a high standard for the

color properties of food samples. Research by Mercali et al. (73) similarly showed that there were no significant ($P > 0.05$) differences in L^*, a^*, and b^* values between OH at frequencies ranging from 0.1 to 100 kHz and conventional heating.

Despite the advantages of a high heating rate, i.e., inactivation of pathogens and maintaining the quality of food, the issue of electrode corrosion and elution into the food should be addressed (74). In the OH process, electrode corrosion occurs through electrodissolution, where metallic electrodes are dissolved (decomposed) into metal ions that have toxic potential (75). Specifically, even a trace amount (125 μg/ml) of titanium dioxide affects cerebral cells and presents potential neurotoxicity (76). Additionally, a number of research studies have shown that accumulating titanium in the body is related to yellow nail syndrome, characterized by yellowing of the nails, respiratory disorders, and lymphedema (77–79). The electrochemical phenomenon of the electrode (M) could be explained as follows (80): $M \rightarrow M^{n+} + ne^-$, where M is metal and e is electron. According to the research of Pataro et al. (81), the flux of metal ions from the electrode to the heating medium was detected, depending on the frequency, applied field strength, electrical conductivity, and pH. They reported that the migration of metal ions increased with increasing applied field strength, acidic conditions, and electrical conductivity of the heating medium. In this study, it was observed that the POH technique using titanium electrodes can prevent electrode corrosion effectively (Table 5). According to Samaranayake et al. (82), POH at lower frequencies and longer pulse widths mitigated the electrochemical reactions, and the concentration of titanium eluted into the heating medium did not exceed the acceptable level according to the published dietary data. Regarding corrosion and eruption of the electrode, electrons are attracted to the electrode and accumulate when voltage is applied to the electrode; therefore, electrical double layers are developed (83). At that moment, the charging current (nonfaradaic current) begins to flow at the surface, where the electrode and material are in contact. In excess of the threshold voltage, a faradaic current, which is current induced by oxidation or reduction, is generated, with an accompanying electrochemical reaction at each electrode surface. The basic principle of impeding electrode corrosion and influx into food products by POH suppresses the faradaic current by changing the direction of the electric current and cutting off voltage before electrons accumulate (84). With regard to electrode materials, Samaranayake and Sastry (85) found that the corrosion rate of titanium electrodes was significantly lower ($P < 0.05$) than that of stainless steel and graphite electrodes regardless of the pH; thus, it could be concluded that titanium is more suitable as a material for the electrode because of its high corrosion resistance. Therefore, this study shows that electrode corrosion is overcome by (i) applying a pulse waveform to OH and (ii) using titanium electrodes.

Integration of the results presented here shows that the POH technique at 80 V_{rms} and a duty ratio of 0.1 is very effective for inactivation of *E. coli* O157:H7, *S.* Typhimurium, and *L. monocytogenes* in soybean curd due to the nonthermal effect (electroporation), thermal effect, and prevention of electrode corrosion. Therefore, we conclude that the POH technique is a novel alternative sterilization process to conventional heating.

MATERIALS AND METHODS

Bacterial culture and suspension preparation. In this research, three strains each of *E. coli* O157:H7 (ATCC 35150, ATCC 43889, and ATCC 43890), *S.* Typhimurium (ATCC 19585, ATCC 43971, and DT 104), and *L. monocytogenes* (ATCC 19114, ATCC 19115, and ATCC 15313) were acquired from the bacterial culture collection of the School of Food Science, Seoul National University (Seoul, South Korea). Each strain was preserved in 0.7 ml of tryptic soy broth (TSB) (Difco, Sparks, MD), mixed with 0.3 ml 50% glycerol at −80°C, and then streaked onto tryptic soy agar (TSA) (Difco, Sparks, MD) and incubated at 37°C for 24 h. The TSA plate was stored at 4°C. A single colony of each strain was inoculated into 5 ml of TSB and then incubated in a shaking incubator (250 rpm) for 24 h at 37°C to obtain working cultures. All the strains were mixed. The mixed culture cocktail was harvested by centrifugation (4,000 × g; 20 min; 4°C), and the supernatant was discarded. The cell pellets acquired were resuspended in 5 ml of sterile 0.2% peptone water (PW) (Becton, Dickinson and Company, Sparks, MD, USA), corresponding to approximately 10^7 to 10^8 CFU/ml.

Sample preparation and inoculation. Soybean curd was purchased from a local grocery store (Seoul, South Korea) and stored in a refrigerator at 4°C before use in the experiments. The soybean curd was cut into 4- by 4- by 3-cm (width, length, and height, respectively) strips using a sterile stainless steel knife and then placed at room temperature until it reached a constant temperature (23 $\pm$ 1°C) before POH treatment. After preparation of the sample, a 10-μl aliquot of the mixed culture cocktail was inoculated into 5 spots on the soybean curd at intervals of 1 cm (Fig. 1B). The depth of each inoculation point was 1.5 cm. The final bacterial population of the sample was 10^8 to 10^9 CFU/ml for *E. coli* O157:H7 and *L. monocytogenes* and 10^7 to 10^8 CFU/ml for *S.* Typhimurium.

Pulsed ohmic heating system and treatment. The fundamental primary composition of the POH system was the same as in a previous study (86). The POH system was composed of a function generator, a power amplifier, a digital oscilloscope, a data logger, a computer, and acrylic plate equipment (Fig. 1A). The function generator produced a variable waveform, with a frequency range of 1 to 10 MHz and a maximum output level of 5 V. The waveform signals produced were transferred to the power amplifier and amplified. The amplified waveform signals were transmitted to two titanium electrodes. During the POH process, the two-channel digital oscilloscope measured the shape of the waveform, frequency, voltage, and electric current. The temperature was measured using three K-type thermocouples placed at 3 points in the soybean curd and recorded every 1 s by the data logger to create a temperature history. The acrylic plate equipment was composed of an acrylic plate and two acrylic supports of the electrodes. The distance between the two electrodes was 4 cm, and the cross-sectional area contacted by the soybean curd was 12 cm². The Benchlink waveform builder program (Keysight Technologies Inc., Santa Rosa, CA, USA) was used to produce a bipolar pulse waveform, which had a period (*T*) of 100 μs. According to equation 2, duty ratios (θ) of 0.1 and 0.05 were adjusted to the width (*t*) of both the positive and negative pulses to 2.5 μs and 5 μs, respectively (82).

$$\theta = \frac{2t}{T} \tag{2}$$

Each of the inoculated samples was treated by POH until the temperature of the sample reached 70, 80, 90, and 100°C, and they were additionally held at 100°C for the time required to increase by 10°C (50, 30, 20, and 15 s at 48, 60, 70, and 80 V_{rms}) at each duty ratio and applied voltage. After the POH treatment, the sample was placed in a stomacher bag (Labplas, Inc., Sainte-Julie, QC, Canada) at room temperature for 5 min to apply residual heat.

Temperature profile measurement. To measure the temperature profile of POH, K-type thermocouples, the data logger, and the computer were used to record the temperature of a sample every second during each treatment. Three temperature measurement points on the samples were selected at 1-cm intervals from the center of the sample surface (Fig. 1B). The temperature was recorded every 20 s and plotted on a graph.

Electrical conductivity measurement. Electrical conductivity (σ), which is the degree of a material's ability to allow the transmittance of an electric charge, is derived from the voltage and current (15). After a two-channel digital oscilloscope was used to measure the voltage and electric current, the electrical conductivity of soybean curd was calculated as follows (equation 3):

$$\sigma = LI/AV \tag{3}$$

where σ is the electrical conductivity (in siemens per centimeter), L is the distance between electrodes (in centimeters), I is the electric current (A_{rms}), A is the cross-sectional area of the sample (in square centimeters), and V is the voltage (V_{rms}).

Viable-cell enumeration. After the pulsed ohmic heating treatment, a sample volume of 48 cm³ was transferred into a sterile stomacher bag containing 192 ml of sterile 0.2% PW. The diluted sample was homogenized for 2 min using a stomacher (Easy Mix; AES Chemunex, Rennes, France). After homogenization, 1-ml sample aliquots were 10-fold serially diluted with 9 ml of sterile 0.2% PW, and the 0.1% diluted and homogenized samples were spread plated onto each selective medium. As selective media, sorbitol MacConkey agar (SMAC) (Difco), xylose lysine deoxycholate agar (XLD) (Difco), and Oxford agar base (OAB) (Difco) with antimicrobial supplement (Bacto Oxford antimicrobial supplement; Difco) were used for enumerating *E. coli* O157:H7, *S.* Typhimurium, and *L. monocytogenes*, respectively. All the spread-plated selective media were incubated at 37°C for 24 h, and then, particular colonies were counted.

Inactivation kinetics modeling and analysis. Inactivation kinetics were analyzed by applying GInaFiT (26, 87, 88) via Microsoft Excel (Microsoft Corp.) to identify the time required to achieve 3- and 5-log-unit reductions (T_{3d} and T_{5d}) of each strain. The equation of the Weibull model is as follows (equation 4):

$$\log N(t) = \log N_0 - \left(\frac{t}{\delta}\right)^\rho \tag{4}$$

where N_0 is the initial inoculum concentration, δ is the time to the first log reduction of the first subpopulation, and ρ is the shape of the inactivation curve. The equation of the Weibull model was converted to calculate and predict T_{3d} and T_{5d} (equation 5):

$$T_{xd} = \delta \times (x)^{\frac{1}{\rho}} \tag{5}$$

Cell membrane potential assessment. The membrane potentials of *E. coli* O157:H7, *S.* Typhimurium, and *L. monocytogenes* were measured using DiBAC$_4$(3) (Molecular Probes, Thermo Fisher Scientific, Waltham, MA, USA) in accordance with previous studies (89–91). To assess the membrane potential of

each pathogen, one strain was inoculated per sample. After POH treatment for 490, 310, 200, and 160 s (maximum treatment times) at 48, 60, 70, and 80 V_{rms}, respectively, the inoculated samples were transferred to a stomacher bag containing PW and homogenized for 2 min. The suspension (40 ml) was transferred a 50-ml conical centrifuge tube (Falcon, Corning, NY, USA) and centrifuged at 1,000 $\times$ g for 15 min to separate the soy milk from the debris of soybean curd. DiBAC$_4$(3) at 2.5 μg/ml in phosphate-buffered saline (PBS) with 4 mM disodium dihydrogen ethylenediaminetetraacetic acid (EDTA-2Na; Junsei Chemical Co., Ltd., Tokyo, Japan) was added to the supernatant to disperse E. coli O157:H7 or S. Typhimurium cells. Then, the suspension was incubated for 15 min at 37°C in a dark room. Compared with E. coli O157:H7 and S. Typhimurium, the suspension of L. monocytogenes was incubated for 2 min at 37°C at 0.5 μg/ml in PBS in a dark room. The samples were centrifuged at 10,000 $\times$ g for 10 min to obtain a cell pellet, excessive DiBAC$_4$(3) dye was removed by washing with PBS, and then centrifugation was performed at 10,000 $\times$ g for 10 min. The cell pellets were resuspended in 1 ml of PBS, and the fluorescence values were determined using a spectrofluorophotometer (Spectramax M2e; Molecular Devices, San Jose, CA, USA) set to an excitation wavelength of 488 nm and an emission wavelength of 525 nm.

Transmission electron microscopy. TEM examination was conducted to visually contrast pathogens treated under different POH treatment conditions. Soybean curd samples inoculated with the mixed culture cocktail were treated by the POH process for 490, 310, 200, and 160 s at 48, 60, 70, and 80 V_{rms}, respectively. Then, samples were transported into stomacher bags containing PW and homogenized for 2 min. A 40-ml suspension was placed into a 50-ml polypropylene conical tube and then centrifuged at 1,000 $\times$ g for 10 min to isolate the debris of soybean curds, such as proteins, lipids, and other substances. A 1-ml aliquot of supernatant was transferred to a 1.5-ml microtube (Axygen, Union City, CA, USA) and centrifuged at 10,000 $\times$ g for 10 min. After discarding the supernatant, modified Karnovsky's fixative, which is composed of 2% paraformaldehyde and 2% glutaraldehyde in 0.05 M sodium cacodylate buffer (pH 7.2), was added to the cell pellet for prefixation at 4°C for 4 h. The prefixed cells were washed in 0.05 M sodium cacodylate buffer (pH 7.2) for 10 min three times. Postfixation was conducted by adding a 1-ml aliquot of 1% osmium tetroxide in 0.05 M sodium cacodylate buffer (pH 7.2) to each sample at 4°C for 2 h, and then the samples were rinsed two times using distilled water at room temperature. The rinsed samples were stained with 0.5% uranyl acetate at 4°C as en bloc staining. After 12 h, the stained cells were dehydrated for 10 min using an ethanol series of 30, 50, 70, 80, 90, and 100% three times. To transition, 100% propylene oxide was added to the dehydrated cells at room temperature for 15 min, and this process was repeated twice. Thereafter, the cells were permeated using 2:1 and 1:1 solutions of propylene oxide and Spurr's resin and 100% Spurr's resin for 2, 12, and 2 h, respectively. Spurr's resin was added to each sample, and the samples were polymerized at 70°C for 24 h. Ultrathin sections were sliced using an Ultramicrotome (MT-X; RMC, Tucson, AZ, USA) and placed on copper single grids. Following this, sections were stained with 2% uranyl acetate for 7 min and Reynold's lead citrate for 7 min in sequence. Finally, the cells were observed through a 120-kV TEM (Libra 120; Carl Zeiss, Germany).

Quality analysis (color and texture measurement). After pulsed ohmic heating treatment for 490, 310, 200, and 160 s at 48, 60, 70, and 80 V_{rms}, respectively, the color values (L^*, a^*, and b^*) of a sample's six surfaces were measured with a Minolta colorimeter (CR400; Minolta Co., Osaka, Japan). L^* indicates lightness, a^* is a measure of redness/greenness, and b^* is a measure of yellowness/blueness (92). Subsequently, each color value was averaged.

The texture properties were measured by TA-XT2 (Stable Micro System, Surrey, United Kingdom) to identify changes in the rheological features of soybean curd after POH treatment. Before the TPA, samples subjected to the POH treatment were kept at room temperature until they reached a constant room temperature. Calibration was performed prior to analysis. The samples were compressed to 50% of the initial height (50% strain) by a 100-mm-diameter compression plate as the probe at a steady cross-head speed of 2.0 mm/s. Using Texture Expert software version 1.22 (Stable Micro System, Surrey, United Kingdom), TPA curves were recorded in real time. Each texture attribute, consisting of hardness, cohesiveness, springiness, gumminess, chewiness, resilience, and adhesiveness, was calculated from the imposed force (N) and area ($N \cdot s$) under the TPA curve (93–95).

Titanium electrode corrosion evaluation. The degree of titanium electrode corrosion was determined by referring to the methods of Lee et al. (17) and Kim et al. (19). After the samples were treated by POH for 490, 310, 200, and 160 s at 48, 60, 70, and 80 V_{rms}, respectively, pretreatment was performed in order to dry the samples to a powder state and to digest the samples in accordance with the EPA 3051 method, which extracts samples using microwave heating with nitric acid (96, 97). Samples (0.5 g) were added to 10 ml nitric acid (Chemitop, Chungbuk, South Korea) and decomposed using the microwave digestion system MARS-6 (CEM Corp., Matthews, NC, USA) for 10 min. The sample with nitric acid was transferred to a fluorocarbon microwave vessel, which was heated in the MARS-6 system for 3 days at 80°C. The heated sample was cooled down and filtered to settle it. Then, an inductively coupled plasma mass spectrometer (820-MS; Varian, Belmont, Australia) was used to conduct the quantitative analysis of the titanium ion concentration in the soybean curd after POH treatment (98–100).

Statistical analysis. All experiments were performed in triplicate. All the data presented in this study were analyzed with Statistical Analysis System software (SAS Institute, Cary, NC, USA). Mean values were separated using Duncan's multiple-range test, and significant differences in the processing treatments were determined at a significance level (P) of 0.05.

REFERENCES

1. Rekha C, Vijayalakshmi G. 2010. Influence of natural coagulants on isoflavones and antioxidant activity of tofu. J Food Sci Technol 47: 38–393. https://doi.org/10.1007/s13197-010-0064-7.
2. Sarkar FH, Li Y. 2003. Soy isoflavones and cancer prevention: clinical science review. Cancer Invest 21:744–757. https://doi.org/10.1081/cnv-120023773.
3. Nguyen HN, Miyagawa N, Miura K, Okuda N, Yoshita K, Arai Y, Nakagawa H, Sakata K, Ojima T, Kadota A, Takashima N, Fujiyoshi A, Ohkubo T, Abbott RD, Okamura T, Okayama A, Ueshima H. 2018. Dietary tofu intake and long-term risk of death from stroke in a general population. Clin Nutr 37:182–188. https://doi.org/10.1016/j.clnu.2016.11.021.
4. Kovats SK, Doyle MP, Tanaka N. 1984. Evaluation of the microbiological safety of tofu. J Food Prot 47:618–622. https://doi.org/10.4315/0362-028X-47.8.618.
5. Ashenafi M. 1994. Microbiological evaluation of tofu and tempeh during processing and storage. Plant Food Hum Nutr 45:183–189. https://doi.org/10.1007/BF01088476.
6. Ananchaipattana C, Hosotani Y, Kawasaki S, Pongswat S, Latiful BM, Isobe S, Inatsu Y. 2012. Bacterial contamination of soybean curd (tofu) sold in Thailand. FSTR 18:843–848. https://doi.org/10.3136/fstr.18.843.
7. Kwon MJ, Rhee MS, Yoon KS. 2019. A risk assessment study of *Bacillus cereus* in packaged tofu at a retail market in Korea. Food Sci Biotechnol 28:339–350. https://doi.org/10.1007/s10068-019-00670-0.
8. Tacket CO, Ballard J, Harris N, Allard J, Nolan C, Quan T, Cohen ML. 1985. An outbreak of Yersinia enterocolitica infections caused by contaminated tofu (soybean curd). Am J Epidemiol 121:705–711. https://doi.org/10.1093/aje/121.5.705.
9. Chai E, Choi E, Guitierrez C, Hochman M, Johnkutty S, Kamel W, Mekles T, Zarnegar R, Ackelsberg J, Balter S. 2013. Botulism associated with home-fermented tofu in two Chinese immigrants—New York City, March-April 2012. MMWR Morb Mortal Wkly Rep 62:529–532.
10. Yamamura K, Sumi N, Egashira Y, Fukuoka I, Motomura S, Tsuchida R. 1992. Food poisoning caused by enteroinvasive *Escherichia coli* (O164: H-): a case in which the causative agent was identified. Kansenshogaku Zasshi 66:761–768. https://doi.org/10.11150/kansenshogakuzasshi1970.66.761.
11. Varghese KS, Pandey M, Radhakrishna K, Bawa A. 2014. Technology, applications and modelling of ohmic heating: a review. J Food Sci Technol 51:2304–2317. https://doi.org/10.1007/s13197-012-0710-3.
12. Goullieux A, Pain J-P. 2014. Ohmic heating, p 399–426, Emerging technologies for food processing. Elsevier, Philadelphia, PA.
13. Mussenbrock T, Brinkmann R, Lieberman M, Lichtenberg A, Kawamura E. 2008. Enhancement of ohmic and stochastic heating by resonance effects in capacitive radio frequency discharges: a theoretical approach. Phys Rev Lett 101:85004. https://doi.org/10.1103/PhysRevLett.101.085004.
14. Yoon S-W, Lee CYJ, Kim K-M, Lee C-H. 2002. Leakage of cellular materials from Saccharomyces cerevisiae by ohmic heating. J Microbiol Biotechnol 12:183–188.
15. Sakr M, Liu S. 2014. A comprehensive review on applications of ohmic heating (OH). Renew Sust Energ Rev 39:262–269. https://doi.org/10.1016/j.rser.2014.07.061.
16. Baysal AH, İçier F. 2010. Inactivation kinetics of *Alicyclobacillus acidoterrestris* spores in orange juice by ohmic heating: effects of voltage gradient and temperature on inactivation. J Food Prot 73:299–304. https://doi.org/10.4315/0362-028X-73.2.299.
17. Lee S-Y, Ryu S, Kang D-H. 2013. Effect of frequency and waveform on inactivation of *Escherichia coli* O157: H7 and *Salmonella enterica* serovar Typhimurium in salsa by ohmic heating. Appl Environ Microbiol 79: 10–17. https://doi.org/10.1128/AEM.01802-12.
18. Park I-K, Ha J-W, Kang D-H. 2017. Investigation of optimum ohmic heating conditions for inactivation of *Escherichia coli* O157: H7, *Salmonella enterica* serovar Typhimurium, and *Listeria monocytogenes* in

apple juice. BMC Microbiol 17:117. https://doi.org/10.1186/s12866-017-1029-z.
19. Kim S-S, Choi W, Kang D-H. 2017. Application of low frequency pulsed ohmic heating for inactivation of foodborne pathogens and MS-2 phage in buffered peptone water and tomato juice. Food Microbiol 63:22–27. https://doi.org/10.1016/j.fm.2016.10.021.
20. Kuphasuk C, Oshida Y, Andres CJ, Hovijitra ST, Barco MT, Brown DT. 2001. Electrochemical corrosion of titanium and titanium-based alloys. J Prosthet Dent 85:195–202. https://doi.org/10.1067/mpr.2001.113029.
21. Koike M, Fujii H. 2001. The corrosion resistance of pure titanium in organic acids. Biomaterials 22:2931–2936. https://doi.org/10.1016/s0142-9612(01)00040-0.
22. Aziz-Kerrzo M, Conroy KG, Fenelon AM, Farrell ST, Breslin CB. 2001. Electrochemical studies on the stability and corrosion resistance of titanium-based implant materials. Biomaterials 22:1531–1539. https://doi.org/10.1016/s0142-9612(00)00309-4.
23. Wang L-J, Li D, Tatsumi E, Liu Z-S, Chen XD, Li L-T. 2007. Application of two-stage ohmic heating to tofu processing. Chem Eng Process 46: 486–490. https://doi.org/10.1016/j.cep.2006.06.017.
24. Lien C-C, Shen Y-C, Ting C-H. 2014. Ohmic heating for tofu making: a pilot study. JACEN 03:7–13. https://doi.org/10.4236/jacen.2014.32B002.
25. Shimoyamada M, Itabashi Y, Sugimoto I, Kanauchi M, Ishida M, Tsuzuki K, Egusa S, Honda Y. 2015. Characterization of soymilk prepared by ohmic heating and the effects of voltage applied. FSTR 21:439–444. https://doi.org/10.3136/fstr.21.439.
26. Buzrul S, Alpas H. 2004. Modeling the synergistic effect of high pressure and heat on inactivation kinetics of *Listeria innocua*: a preliminary study. FEMS Microbiol Lett 238:29–36. https://doi.org/10.1016/j.femsle.2004.07.011.
27. Chen H, Hoover DG. 2004. Use of Weibull model to describe and predict pressure inactivation of *Listeria monocytogenes* Scott A in whole milk. Innov Food Sci Emerg 5:269–276. https://doi.org/10.1016/j.ifset.2004.03.002.
28. Somavat R, Mohamed HM, Sastry SK. 2013. Inactivation kinetics of *Bacillus coagulans* spores under ohmic and conventional heating. LWT Food Sci Technol 54:194–198. https://doi.org/10.1016/j.lwt.2013.04.004.
29. Sun H, Masuda F, Kawamura S, Himoto JI, Asano K, Kimura T. 2011. Effect of electric current of ohmic heating on nonthermal injury to *Streptococcus thermophilus* in milk. J Food Process Eng 34:878–892. https://doi.org/10.1111/j.1745-4530.2009.00515.x.
30. Kaur N, Singh A. 2016. Ohmic heating: concept and applications. Crit Rev Food Sci Nutr 56:2338–2351. https://doi.org/10.1080/10408398.2013.835303.
31. Cappato LP, Ferreira MVS, Guimaraes JT, Portela JB, Costa ALR, Freitas MQ, Cunha RL, Oliveira CAF, Mercali GD, Marzack LDF, Cruz AG. 2017. Ohmic heating in dairy processing: relevant aspects for safety and quality. Trends Food Sci Technol 62:104–112. https://doi.org/10.1016/j.tifs.2017.01.010.
32. Piette G, Buteau ML, Halleux D, Chiu L, Raymond Y, Ramaswamy HS, Dostie M. 2006. Ohmic cooking of processed meats and its effects on product quality. J Food Sci 69:fep71–fep78. https://doi.org/10.1111/j.1365-2621.2004.tb15512.x.
33. Knirsch MC, Dos Santos CA, de Oliveira Soares AAM, Penna T. 2010. Ohmic heating: a review. Trends Food Sci Technol 21:436–441. https://doi.org/10.1016/j.tifs.2010.06.003.
34. Darvishi H, Khostaghaza MH, Najafi G. 2013. Ohmic heating of pomegranate juice: electrical conductivity and pH change. J Saudi Soc Agr Sci 12:101–108. https://doi.org/10.1016/j.jssas.2012.08.003.
35. El Darra N, Grimi N, Vorobiev E, Louka N, Maroun R. 2013. Extraction of polyphenols from red grape pomace assisted by pulsed ohmic heating. Food Bioprocess Technol 6:1281–1289. https://doi.org/10.1007/s11947-012-0869-7.

36. Darvishi H, Hosainpour A, Nargesi F. 2012. Ohmic heating behaviour and electrical conductivity of tomato paste. J Nutr Food Sci 2:1–5.

37. Bozkurt H, Icier F. 2012. Ohmic thawing of frozen beef cuts. J Food Process Eng 35:16–36. https://doi.org/10.1111/j.1745-4530.2009.00569.x.

38. Nodeh IR, Serajzadeh S, Kokabi AH. 2008. Simulation of welding residual stresses in resistance spot welding, FE modeling and X-ray verification. J Mater Process Tech 205:60–69. https://doi.org/10.1016/j.jmatprotec.2007.11.104.

39. Fan G, Gao L, Hussain G, Wu Z. 2008. Electric hot incremental forming: a novel technique. Int J Mach Tool Manu 48:1688–1692. https://doi.org/10.1016/j.ijmachtools.2008.07.010.

40. Jin Y, Cheng Y-D, Fukuoka M, Sakai N. 2015. Electrical conductivity of yellowtail (Seriola quinqueradiata) fillets during ohmic heating. Food Bioprocess Technol 8:1904–1913. https://doi.org/10.1007/s11947-015-1546-4.

41. Sarang S, Sastry SK, Knipe L. 2008. Electrical conductivity of fruits and meats during ohmic heating. J Food Eng 87:351–356. https://doi.org/10.1016/j.jfoodeng.2007.12.012.

42. Castro I, Teixeira JA, Salengke S, Sastry SK, Vicente AA. 2004. Ohmic heating of strawberry products: electrical conductivity measurements and ascorbic acid degradation kinetics. Innov Food Sci Emerg 5:27–36. https://doi.org/10.1016/j.ifset.2003.11.001.

43. Pereira R, Martins J, Mateus C, Teixeira J, Vicente A. 2007. Death kinetics of Escherichia coli in goat milk and Bacillus licheniformis in cloudberry jam treated by ohmic heating. Chem Pap 61:121–126.

44. Sun H, Kawamura S, Himoto J-I, Itoh K, Wada T, Kimura T. 2008. Effects of ohmic heating on microbial counts and denaturation of proteins in milk. FSTR 14:117–123. https://doi.org/10.3136/fstr.14.117.

45. Mason D, Lopez-Amoros R, Allman R, Stark J, Lloyd D. 1995. The ability of membrane potential dyes and calcafluor white to distinguish between viable and non-viable bacteria. J Appl Bacteriol 78:309–315. https://doi.org/10.1111/j.1365-2672.1995.tb05031.x.

46. Novo DJ, Perlmutter NG, Hunt RH, Shapiro HM. 2000. Multiparameter flow cytometric analysis of antibiotic effects on membrane potential, membrane permeability, and bacterial counts of Staphylococcus aureus and Micrococcus luteus. Antimicrob Agents Chemother 44:827–834. https://doi.org/10.1128/AAC.44.4.827-834.2000.

47. Ehrenberg B, Farkas DL, Fluhler EN, Lojewska Z, Loew LM. 1987. Membrane potential induced by external electric field pulses can be followed with a potentiometric dye. Biophys J 51:833–837. https://doi.org/10.1016/S0006-3495(87)83410-0.

48. Hülsheger H, Potel J, Niemann E-G. 1983. Electric field effects on bacteria and yeast cells. Radiat Environ Biophys 22:149–162. https://doi.org/10.1007/BF01338893.

49. Dimitrov D. 1984. Electric field-induced breakdown of lipid bilayers and cell membranes: a thin viscoelastic film model. J Membr Biol 78:53–60. https://doi.org/10.1007/BF01872532.

50. Toepfl S, Heinz V, Knorr D. 2007. High intensity pulsed electric fields applied for food preservation. Chem Eng Proces 46:537–546. https://doi.org/10.1016/j.cep.2006.07.011.

51. Benarroch JM, Asally M. 2020. The microbiologist's guide to membrane potential dynamics. Trends Microbiol 28:304–314. https://doi.org/10.1016/j.tim.2019.12.008.

52. Maloney PC, Kashket E, Wilson TH. 1974. A protonmotive force drives ATP synthesis in bacteria. Proc Natl Acad Sci U S A 71:3896–3900. https://doi.org/10.1073/pnas.71.10.3896.

53. Poole RJ. 1978. Energy coupling for membrane transport. Annu Rev Plant Physiol 29:437–460. https://doi.org/10.1146/annurev.pp.29.060178.002253.

54. Maher MP, Wu N-T, Ao H. 2007. pH-insensitive FRET voltage dyes. J Biomol Screen 12:656–667. https://doi.org/10.1177/1087057107302113.

55. Adams DS, Levin M. 2012. Measuring resting membrane potential using the fluorescent voltage reporters DiBAC4 (3) and CC2-DMPE. Cold Spring Harb Protoc 2012:459–464. https://doi.org/10.1101/pdb.prot067702.

56. Sastry S. 2009. Ohmic heating. Food Eng 3:37.

57. Donsì F, Ferrari G, Pataro G. 2010. Applications of pulsed electric field treatments for the enhancement of mass transfer from vegetable tissue. Food Eng Rev 2:109–130. https://doi.org/10.1007/s12393-010-9015-3.

58. Lee J-Y, Kim S-S, Kang D-H. 2015. Effect of pH for inactivation of Escherichia coli O157: H7, Salmonella Typhimurium and Listeria monocytogenes in orange juice by ohmic heating. LWT Food Sci Technol 62:83–88. https://doi.org/10.1016/j.lwt.2015.01.020.

59. de Quadros Rodrigues R, Dalmás M, Chemello Muller D, Dambróz Escobar D, Campani Pizzato A, Mercali GD, Tondo EC. 2018. Evaluation of nonthermal effects of electricity on inactivation kinetics of Staphylococcus aureus and Escherichia coli during ohmic heating of infant formula. J Food Saf 38:e12372. https://doi.org/10.1111/jfs.12372.

60. Clements AN. 2011. The biology of mosquitoes, vol 3. Viral, arboviral, and bacterial pathogens. CABI, Wallingford, United Kingdom.

61. Mai-Prochnow A, Clauson M, Hong J, Murphy AB. 2016. Gram positive and Gram negative bacteria differ in their sensitivity to cold plasma. Sci Rep 6:38610. https://doi.org/10.1038/srep38610.

62. Park I-K, Kang D-H. 2013. Effect of electropermeabilization by ohmic heating for inactivation of Escherichia coli O157:H7, Salmonella enterica serovar Typhimurium, and Listeria monocytogenes in buffered peptone water and apple juice. Appl Environ Microbiol 79:7122–7129. https://doi.org/10.1128/AEM.01818-13.

63. Lee SY, Sagong HG, Ryu S, Kang DH. 2012. Effect of continuous ohmic heating to inactivate Escherichia coli O157:H7, Salmonella Typhimurium and Listeria monocytogenes in orange juice and tomato juice. J Appl Microbiol 112:723–731. https://doi.org/10.1111/j.1365-2672.2012.05247.x.

64. Anderson DR. 2008. Ohmic heating as an alternative food processing technology. MSc thesis. Kansas University, Manhattan, KS.

65. Hashim I, Khalil A, Afifi H. 2009. Quality characteristics and consumer acceptance of yogurt fortified with date fiber. J Dairy Sci 92:5403–5407. https://doi.org/10.3168/jds.2009-2234.

66. Kamizake NKK, Silva LCP, Prudencio SH. 2018. Impact of soybean aging conditions on tofu sensory characteristics and acceptance. J Sci Food Agric 98:1132–1139. https://doi.org/10.1002/jsfa.8564.

67. Obatolu VA. 2008. Effect of different coagulants on yield and quality of tofu from soymilk. Eur Food Res Technol 226:467–472. https://doi.org/10.1007/s00217-006-0558-8.

68. Di Monaco R, Cavella S, Masi P. 2008. Predicting sensory cohesiveness, hardness and springiness of solid foods from instrumental measurements. J Texture Studies 39:129–149. https://doi.org/10.1111/j.1745-4603.2008.00134.x.

69. Montejano J, Hamann D, Lanier T. 1985. Comparison of two instrumental methods with sensory texture of protein gels. J Texture Studies 16:403–424. https://doi.org/10.1111/j.1745-4603.1985.tb00705.x.

70. Szczesniak AS. 1963. Classification of textural characteristics. J Food Sci 28:385–389. https://doi.org/10.1111/j.1365-2621.1963.tb00215.x.

71. Hashizume K, Maeda M, Watanabe T. 1978. Relationship of heating and cooling condition to hardness of tofu. J Food Sci Technol 25:387–391. https://doi.org/10.3136/nskkk1962.25.387.

72. Furukawa T, Ohta S, Yamamoto A. 1980. Texture-structure relationships in heat-induced soy protein gels. J Texture Studies 10:333–346. https://doi.org/10.1111/j.1745-4603.1980.tb00864.x.

73. Mercali GD, Schwartz S, Marczak LDF, Tessaro IC, Sastry S. 2014. Ascorbic acid degradation and color changes in acerola pulp during ohmic heating: effect of electric field frequency. J Food Eng 123:1–7. https://doi.org/10.1016/j.jfoodeng.2013.09.011.

74. Zhao Y, Kolbe E, Flugstad B. 1999. A method to characterize electrode corrosion during ohmic heating. J Food Proc Eng 22:81–89. https://doi.org/10.1111/j.1745-4530.1999.tb00472.x.

75. Samaranayake CP. 2003. Electrochemical reactions during ohmic heating. Ohio State University. Columbus, OH.

76. Coccini T, Grandi S, Lonati D, Locatelli C, De Simone U. 2015. Comparative cellular toxicity of titanium dioxide nanoparticles on human astrocyte and neuronal cells after acute and prolonged exposure. Neurotoxicology 48:77–89. https://doi.org/10.1016/j.neuro.2015.03.006.

77. Berglund F, Carlmark B. 2011. Titanium, sinusitis, and the yellow nail syndrome. Biol Trace Elem Res 143:1–7. https://doi.org/10.1007/s12011-010-8828-5.

78. Ataya A, Kline KP, Cope J, Alnuaimat H. 2015. Titanium exposure and yellow nail syndrome. Respir Med Case Rep 16:146–147. https://doi.org/10.1016/j.rmcr.2015.10.002.

79. Vignes S, Baran R. 2017. Yellow nail syndrome: a review. Orphanet J Rare Dis 12:42. https://doi.org/10.1186/s13023-017-0594-4.

80. Kamer PC, Vogt D, Thybaut JW. 2017. Contemporary catalysis: science, technology and applications. Royal Society of Chemistry, London, United Kingdom.

81. Pataro G, Barca GM, Pereira RN, Vicente AA, Teixeira JA, Ferrari G. 2014. Quantification of metal release from stainless steel electrodes during conventional and pulsed ohmic heating. Innov Food Sci Emerg 21:66–73. https://doi.org/10.1016/j.ifset.2013.11.009.

82. Samaranayake CP, Sastry SK, Zhang H. 2005. Pulsed ohmic heating—a

novel technique for minimization of electrochemical reactions during processing. J Food Sci 70:e460–5. https://doi.org/10.1111/j.1365-2621.2005.tb11515.x.

83. Sawyer DT, Sobkowiak A, Roberts JL. 1995. Electrochemistry for chemists. Wiley, New York, NY.

84. Sastry S, Abdelrahim K, Ramaswamy HS, Marcotte M. 2014. Ohmic heating in food processing. CRC Press, Boca Raton, FL.

85. Samaranayake CP, Sastry SK. 2005. Electrode and pH effects on electrochemical reactions during ohmic heating. J Electroanal Chem 577:125–135. https://doi.org/10.1016/j.jelechem.2004.11.026.

86. Kim SS, Kang DH. 2015. Effect of milk fat content on the performance of ohmic heating for inactivation of *Escherichia coli* O157: H7, *Salmonella enterica* serovar Typhimurium and *Listeria monocytogenes*. J Appl Microbiol 119:475–486. https://doi.org/10.1111/jam.12867.

87. Geeraerd A, Valdramidis V, Van Impe J. 2005. GInaFiT, a freeware tool to assess non-log-linear microbial survivor curves. Int J Food Microbiol 102:95–105. https://doi.org/10.1016/j.ijfoodmicro.2004.11.038.

88. Kim D-K, Kim S-J, Kang D-H. 2017. Inactivation modeling of human enteric virus surrogates, MS2, Qβ, and ΦX174, in water using UVC-LEDs, a novel disinfecting system. Food Res Int 91:115–123. https://doi.org/10.1016/j.foodres.2016.11.042.

89. Kim D-K, Kim S-J, Kang D-H. 2017. Bactericidal effect of 266 to 279 nm wavelength UVC-LEDs for inactivation of Gram positive and Gram negative foodborne pathogenic bacteria and yeasts. Food Res Int 97:280–287. https://doi.org/10.1016/j.foodres.2017.04.009.

90. Kim S-S, Kang D-H. 2017. Combination treatment of ohmic heating with various essential oil components for inactivation of food-borne pathogens in buffered peptone water and salsa. Food Control 80:29–36. https://doi.org/10.1016/j.foodcont.2017.04.001.

91. Kim D-K, Kang D-H. 2018. Elevated inactivation efficacy of a pulsed UVC light-emitting diode system for foodborne pathogens on selective media and food surfaces. Appl Environ Microbiol 84:e01340-18. https://doi.org/10.1128/AEM.01340-18.

92. Leon K, Mery D, Pedreschi F, Leon J. 2006. Color measurement in *L* *a* *b* units from RGB digital images. Food Res Int 39:1084–1091. https://doi.org/10.1016/j.foodres.2006.03.006.

93. Peleg M. 2008. Texture profile analysis parameters obtained by an Instron universal testing machine. J Food Sci 41:721–722. https://doi.org/10.1111/j.1365-2621.1976.tb00710_41_3.x.

94. Bourne M, Kenny J, Barnard J. 1978. Computer-assisted readout of data from texture profile analysis curves 1. J Texture Studies 9:481–494. https://doi.org/10.1111/j.1745-4603.1978.tb01219.x.

95. Cruz RM, Khmelinskii I, Vieira M. 2014. Methods in food analysis. CRC Press, Boca Raton, FL.

96. U.S. Environmental Protection Agency. 1995. Method 3051: microwave assisted acid digestion of sediments, sludges, soils, and oils, p 1–30. *In* Test methods for evaluating solid waste: physical/chemical methods. U.S. Environmental Protection Agency, Washington, DC.

97. Element C. 2007. Method 3051A: microwave assisted acid digestion of sediments, sludges, soils, and oils. Z Anal Chem 111:362–366.

98. Weir A, Westerhoff P, Fabricius L, Hristovski K, Von Goetz N. 2012. Titanium dioxide nanoparticles in food and personal care products. Environ Sci Technol 46:2242–2250. https://doi.org/10.1021/es204168d.

99. Lin Q-B, Li H, Zhong H-N, Zhao Q, Xiao D-H, Wang Z-W. 2014. Migration of Ti from nano-TiO₂-polyethylene composite packaging into food simulants. Food Addit Contam 31:1284–1290. https://doi.org/10.1080/19440049.2014.907505.

100. Lim J-H, Bae D, Fong A. 2018. Titanium dioxide in food products: quantitative analysis using ICP-MS and Raman spectroscopy. J Agric Food Chem 66:13533–13540. https://doi.org/10.1021/acs.jafc.8b06571.